Proc. Natl. Acad. Sci. USA
Vol. 91, pp. 6649–6653, July 1994
Plant Biology

Differential regulation of an auxin-producing nitrilase gene family in *Arabidopsis thaliana*

(indole-3-acetic acid/indole-3-acetonitrile/phytohormone/β-glucuronidase)

BONNIE BARTEL* AND GERALD R. FINK*†

*Whitehead Institute for Biomedical Research and †Department of Biology, Massachusetts Institute of Technology, Nine Cambridge Center, Cambridge, MA 02142

Contributed by Gerald R. Fink, March 23, 1994

ABSTRACT **Nitrilases (nitrile aminohydrolase, EC 3.5.5.1) convert nitriles to carboxylic acids. We report the cloning, characterization, and expression patterns of four *Arabidopsis thaliana* nitrilase genes (*NIT1–4*), one of which was previously described [Bartling, D., Seedorf, M., Mithöfer, A. & Weiler, E. W. (1992) *Eur. J. Biochem.* 205, 417–424]. The nitrilase genes encode very similar proteins that hydrolyze indole-3-acetonitrile to the phytohormone indole-3-acetic acid *in vitro*, and three of the four genes are tandemly arranged on chromosome III. Northern analysis using gene-specific probes and analysis of transgenic plants containing promoter–reporter gene fusions indicate that the four genes are differentially regulated. *NIT2* expression is specifically induced around lesions caused by bacterial pathogen infiltration. The sites of nitrilase expression may represent sites of auxin biosynthesis in *A. thaliana*.**

Auxins are phytohormones that affect many plant processes, including cell division, cell elongation, tropisms, and apical dominance (1). Despite the importance of auxins in plant growth and development, the pathway(s) of auxin biosynthesis has not been definitively determined in any plant. Indole-3-acetonitrile (IAN) appears to be the immediate precursor of the most abundant auxin, indole-3-acetic acid (IAA), in the Brassicaceae family (2). A nitrilase activity (nitrile aminohydrolase, EC 3.5.5.1) that hydrolyzes IAN to IAA has been detected in a variety of plants (3) and has been partially purified from *Brassica campestris* (4). A cDNA homologous to microbial nitrilases was recently cloned from *Arabidopsis thaliana* (5); the enzyme encoded by this gene converts IAN to IAA when expressed in *Escherichia coli* (5).

Recent work measuring auxin levels in tryptophan biosynthetic mutants has shown that, in *A. thaliana* and maize, the bulk of IAA is derived not from tryptophan itself, as was long supposed, but rather from an unidentified precursor of tryptophan (6, 7). Interestingly, the *A. thaliana trp2* and *trp3* mutants, which are blocked in the final and penultimate steps of tryptophan biosynthesis, respectively (8, 9), accumulate not only IAA but also IAN (6). This result is consistent with IAN being a precursor of IAA in *A. thaliana*.

Nitrilase activity may directly influence levels of IAA in the plant. To identify potential sites of IAA production, we examined the regulation of nitrilase gene expression. We found that *A. thaliana* has three nitrilase genes‡ in addition to the one described previously. These four genes show different patterns of expression during development and in response to pathogen invasion.

MATERIALS AND METHODS

Cultivars and Strains. *A. thaliana* ecotype Columbia (Col-0) was the source for DNA and RNA, ecotype Nossen (No-0) was used for transformation, and mapping was carried out using crosses between Col-0 and Landsberg (La-0). *E. coli* strains DH5α and JM101 were used for plasmid construction, and LE392 was the host for λ derivatives. *Agrobacterium tumefaciens* strain LBA4404 (10) was transformed with plasmids by electroporation.

DNA and RNA Methods. Standard techniques for DNA analysis, cloning, and sequencing were performed (11). RNA was analyzed as described (12). Membranes were hybridized to ^{32}P-labeled (Prime Time C; International Biotechnologies) DNA fragments overnight at 65°C (13), followed by washing at room temperature with 0.2× SSC/0.1% SDS (11).

Nitrilase Cloning. A 1-kb *NIT1* cDNA PCR product (obtained using the primers 5′-GCTCTAGATATGTCTAGTACTAAAGATATGTC-3′ and 5′-CGTCTAGATTACTATTTGTTTGAGTCATCCTCAGC-3′) was used to probe an *A. thaliana* cDNA library (14) by plaque hybridization at high stringency. Fifteen *NIT1* cDNAs, 2 *NIT2* cDNAs, and 2 *NIT3* cDNAs were recovered from ≈10^5 plaques. The *NIT1* cDNA was used to probe a λGEM11-based *A. thaliana* genomic library (a gift of J. Mulligan and R. Davis, Stanford University) and positive clones were placed in two groups, one containing eight clones spanning *NIT1*, *NIT2*, and *NIT3* and the second containing four clones carrying a fourth gene, *NIT4*. A fragment from the *NIT4* coding region was used to probe a second *A. thaliana* cDNA library (15), and 20 *NIT1* cDNAs, 6 *NIT2* cDNAs, 3 *NIT3* cDNAs, and 3 *NIT4* cDNAs were recovered from 3 × 10^4 colonies. The longest cDNA isolated for each gene was sequenced on both strands.

***E. coli* Expression.** Nitrilase cDNAs cloned in pKK223-3 (Pharmacia) were transformed into JM101. Expression from the *trp-lac* promoter was induced in exponentially growing cells by addition of isopropyl β-D-thiogalactopyranoside to 1 mM. After 2 hr at 36°C, 3 ml of cells was harvested by centrifugation, resuspended in 80 μl of lysis buffer (200 mM Hepes, pH 7.0/1 mM EDTA/5 mM 2-mercaptoethanol/0.05% Triton X-100), and lysed by freezing and thawing. An equal volume of 10 mM IAN in lysis buffer was added. After 16 hr at 30°C, 1 μl of each reaction mixture was spotted on a TLC plate (0.25-mm Kieselgel 60; Merck) alongside standards. The plate was developed with 49.5% (vol/vol) hexane/49.5% (vol/vol) ethyl acetate/1% (vol/vol) acetic acid and visualized with Ehrlich's reagent (Sigma). In this system, retardation factors are 0.69 for IAN, 0.36 for IAA, and 0.07 for indole-3-acetamide. All four *A. thaliana* nitrilases converted IAN to IAA and indole-3-acetamide. The enzymes did not utilize indole-3-acetamide as a substrate. Neither boiled extract, JM101 containing only vector, nor cDNAs in the antisense orientation were active.

The publication costs of this article were defrayed in part by page charge payment. This article must therefore be hereby marked "*advertisement*" in accordance with 18 U.S.C. §1734 solely to indicate this fact.

Abbreviations: IAA, indole-3-acetic acid; IAN, indole-3-acetonitrile; GUS, β-glucuronidase.

‡The sequences reported in this paper have been deposited in the GenBank data base [accession nos. U09958 (*NIT2*), U09959 (*NIT3*), and U09961 (*NIT4*)].

Mapping. The *NIT1,2,3* gene cluster was mapped by performing PCR with the primers 5′-GCGAATTCGGTTGTGATTCGTCAG-3′ and 5′-GCAGTACTAGACATATCAACTCG-3′, which resulted in amplification of a 1.8-kb product from Col-0 and a 1.9-kb product from La-0 genomic DNA. The map distances shown in Fig. 2 were calculated (16) from the segregation of 60 F_2 individuals (*NIT1,2,3* to *GL1*) and 65 recombinant inbred lines (17) (*NIT1,2,3* to m249). *NIT4* was mapped by developing a PCR-based marker (18). PCR using the primers 5′-CGTTTCTTGTTGCATGGATCCATGAGAGAATCAG-3′ and 5′-CAACTCCACATCCGTCGGCG-3′ resulted in amplification of a 2-kb product that contained an *Mbo* II restriction fragment length polymorphism between the ecotypes Col-0 and La-0. The map distances shown in Fig. 2 were calculated from the segregation of 36 F_2 individuals (*NIT4* to *trp1*) and 53 recombinant inbred lines (17) (*NIT4* to m291).

Promoter–β-Glucuronidase (GUS) Fusions. The 1.9-kb *Bgl* II–*Sca* I fragment of the *NIT1* 5′ region was cloned into pBI101.3 (19) to give a translational fusion of the first three codons of *NIT1* to the *E. coli uidA* gene, which encodes GUS. A *Bam*HI site (underlined) was introduced by mutagenesis (with the oligonucleotide 5′-CGGAGTGTTTTCTGAAGGATCCATTTTTTCTGTTTTAAC-3′) at the second codon of *NIT2*, and the 2.5-kb *Bam*HI–*Hin*dIII fragment of the *NIT2* promoter was cloned into pBI101.2 (19) to give a translational fusion of the first codon of *NIT2* to *uidA*. The 3-kb *Xba* I–*Xho* I fragment of the *NIT3* 5′ region was cloned into pBI101.2 to give a transcriptional fusion (ending at −5 bp from the ATG) of the *NIT3* promoter to *uidA*. The 2-kb region 5′ of the *NIT4* ATG (obtained by PCR using *NIT4* mapping primers) was cloned into pBI101.2 to give a translational fusion of the first codon of *NIT4* to *uidA*.

***A. thaliana* Transformation.** Root explants were transformed and regenerated essentially as described (20). T_1 seeds from primary transformed plants (T_0) were spread on PNS (21) plates containing kanamycin at 10 μg/ml, and resistant plants were transferred to soil and allowed to self-pollinate. Plants homozygous for the transgene were identified by testing segregation of kanamycin resistance in the T_2 or T_3 generation. Lines with abnormally large seeds were considered to have aberrant ploidy and were discarded. Ten of 10 NIT1–GUS, 9 of 11 NIT2–GUS, 3 of 4 NIT3–GUS, and 2 of 5 NIT4–GUS homozygous diploid lines exhibited GUS staining.

Histochemical Localization of GUS. GUS activity was localized by staining with 0.1 (NIT1–GUS) or 0.5 (NIT2–, NIT3–, and NIT4–GUS) mg of 5-bromo-4-chloro-3-indolyl-β-D-glucuronide (X-Gluc; Gold Biotechnology, St. Louis) per ml in X-Gluc buffer (22) containing 0.01% Triton X-100. After three rounds of vacuum infiltration, staining reactions proceeded overnight at 37°C in the dark. Chlorophyll was removed by incubation in ethanol, and tissue was rehydrated in water and mounted in 50% (vol/vol) glycerol/0.01% Triton X-100 for photography.

RESULTS

Using a previously cloned (5) cDNA (referred to here as *NIT1*) as a probe, we cloned by hybridization four nitrilase (*NIT*) genes from *A. thaliana* genomic and cDNA libraries (see *Materials and Methods*). Based on cDNA abundance, *NIT1* is likely to encode the predominant nitrilase isozyme, whereas *NIT2*, *NIT3*, and *NIT4* are approximately 4- to 8-fold less abundant. The cDNAs were subcloned into an *E. coli* expression vector, and extracts from the resultant transformants hydrolyzed IAN to IAA (see *Materials and Methods*), indicating that *NIT1*, *NIT2*, *NIT3*, and *NIT4* each encode functional nitrilase isozymes.

A comparison of the four *A. thaliana* nitrilases with microbial nitrilases (Fig. 1) shows that the 38-kDa NIT1, NIT2, and NIT3 proteins are ≈85% identical to each other, whereas the 39-kDa NIT4 protein is only ≈65% identical to NIT1, NIT2, and NIT3. Each *A. thaliana* nitrilase is ≈25% similar to bacterial nitrilases.

The *NIT1*, *NIT2*, and *NIT3* genes were found on overlapping genomic clones and are arranged in a tandem array in the genome spanning ≈12 kb (Fig. 2*A*). All three genes are transcribed in the same direction. This nitrilase gene cluster was mapped to chromosome III between *GL1* and m249, and *NIT4* was mapped to chromosome V between *trp1* (*PAT1*) and m291 (Fig. 2*B*; see *Materials and Methods*).

Northern analysis of RNA prepared from 5-week-old plants indicated that the *NIT* genes are expressed in different tissues (Fig. 3). *NIT1* was highly expressed in rosette leaves, with lower levels detected in other tissues. *NIT2* was highly expressed in siliques, *NIT3* was preferentially expressed in roots, and *NIT4* mRNA was most abundant in green tissues (leaves, stems, and siliques).

To locate these expression differences more exactly, we constructed transgenic plants containing reporter gene fu-

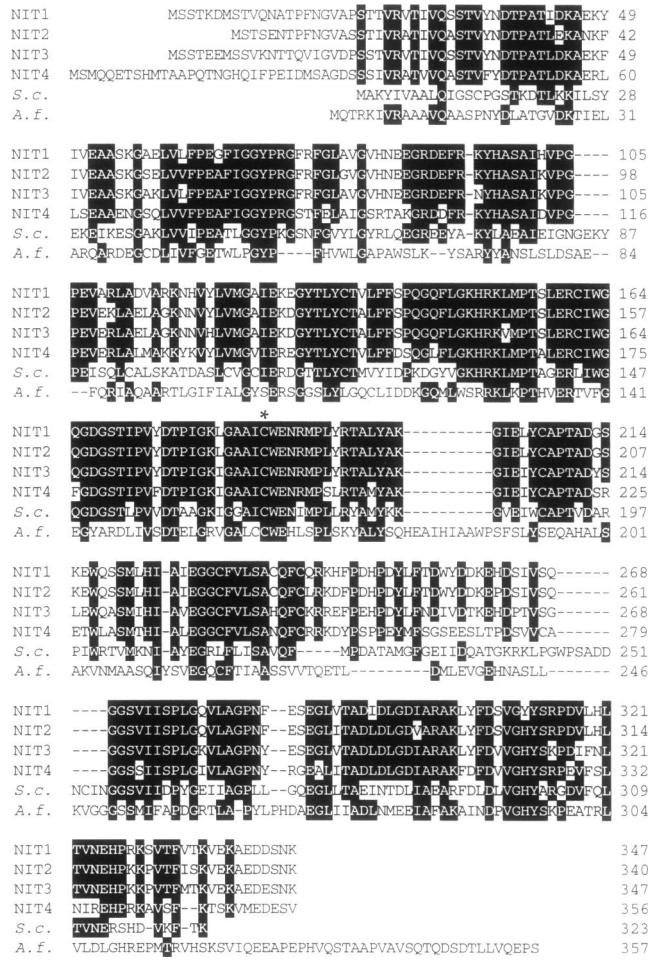

FIG. 1. Alignment of *A. thaliana* and microbial nitrilases. Sequences shown are NIT1 (5), NIT2, NIT3, and NIT4 from *A. thaliana*; an open reading frame from *Saccharomyces cerevisiae* (*S.c.*; altered by changing an A to a G at codon 199 and inserting a G at codon 297 to maintain the homologous open reading frame; GenBank accession no. X66132); and a nitrilase from *Alcaligenes faecalis* JM3 [*A.f.*, (23)]. Sequences were aligned with the MEGALIGN program (DNAstar, Madison, WI) using the Clustal method (24). Amino acid residues identical in at least four of the six sequences are boxed, an asterisk denotes a putative active site cysteine (23, 25, 26), and hyphens indicate gaps introduced to maximize alignment.

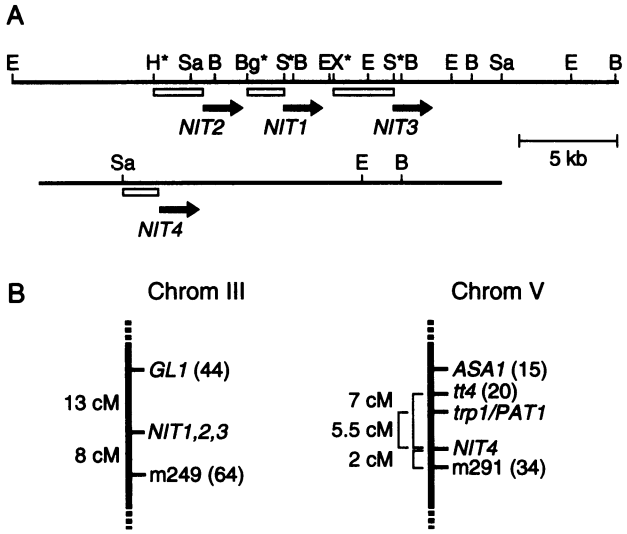

FIG. 2. Genomic organization of the nitrilase loci. (*A*) Horizontal lines represent cloned genomic DNA, arrows represent nitrilase coding sequences and the direction of transcription, and open rectangles represent promoter regions used to make reporter gene fusions (see *Materials and Methods*). B, *Bam*HI; Bg, *Bgl* II; E, *Eco*RI; H, *Hin*dIII; Sa, *Sal* I; S, *Sca* I; X, *Xba* I. Sites marked with an asterisk are not necessarily unique in the region shown. (*B*) Map positions. Numbers in parentheses are integrated map positions from AAtDB, an *Arabidopsis thaliana* data base, Release 5 (27). Numbers to the left of the line represent map distances in centimorgans (cM) calculated from our data. Chrom, chromosome.

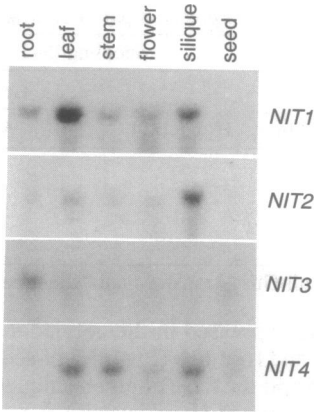

FIG. 3. Tissue specificity of nitrilase gene expression. Five micrograms of total RNA prepared from roots (root), rosette leaves (leaf), stems of flowering stalks (stem), immature and fully opened flowers (flower), green seed pods (silique), and mature dry seeds (seed) of 5-week-old *A. thaliana* plants (12) were hybridized to the following cDNA-derived gene-specific probes: *NIT1*, 200-bp 3′ noncoding *Fok* I–*Dra* I fragment; *NIT2*, 230-bp 3′ noncoding fragment amplified by PCR (using the primers 5′-GCGAATTCGGTTGTGATTCGTCAG-3′ and 5′-GCGAATTCATAATAATTGGCTACATGG-3′); *NIT3*, 267-bp 3′ noncoding *Acc* I–*Xba* I fragment; *NIT4*, 5′ 210 bp (130 bp of 5′ noncoding and 75 bp of coding sequence). The *NIT1* filter was exposed for 12 hr and the other filters were exposed for 6 days.

sions. The promoter region of each gene (Fig. 2*A*) was cloned upstream of the *E. coli* reporter gene *uidA*, which encodes GUS, and these constructs were used to transform *A. thaliana*. In 3-day-old transgenic seedlings, NIT1–GUS was detected most strongly in the hypocotyl near its junction with the root and was also found in cotyledons and root tips (Fig. 4*A*). In 12-day-old seedlings, NIT1–GUS was detected in the distal tip of leaves that were not yet fully expanded (Fig. 4*B*) and root tips (Fig. 4 *E* and *F*). Mature plants expressed NIT1–GUS in stems, cauline leaves, stipules, sepals, anthers (Fig. 4*C*), and at the tip and the base of green siliques (Fig. 4*D*).

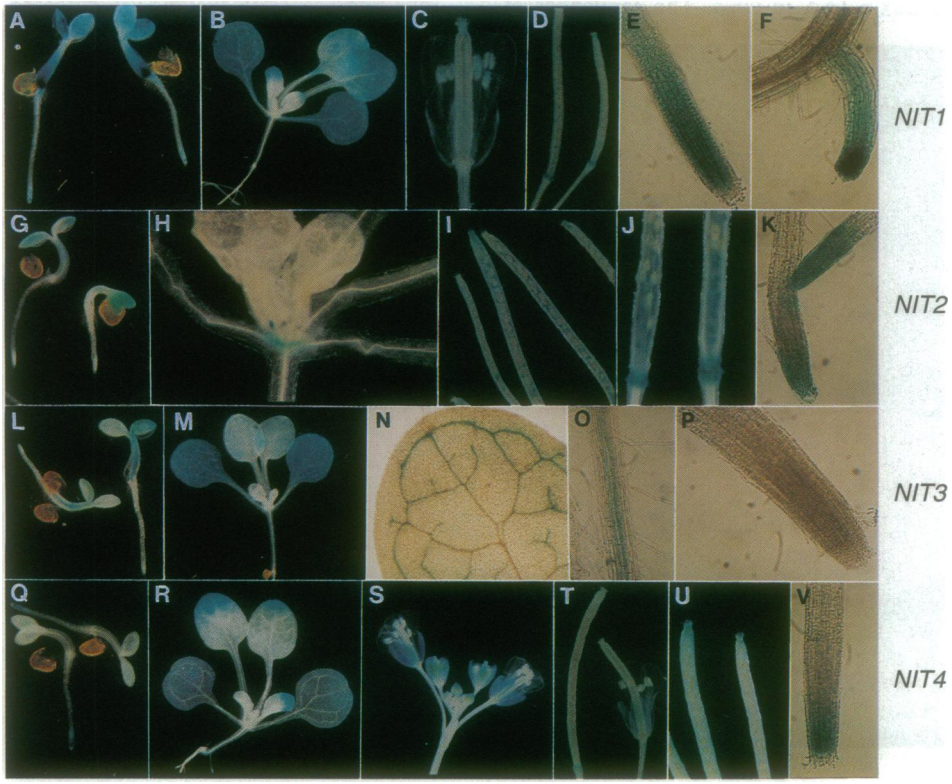

FIG. 4. Histochemical localization of nitrilase expression. Homozygous transgenic lines containing promoter–GUS fusions were stained for GUS activity after growing on PNS (21) for 3 (*A*, *G*, *L*, and *Q*) or 12 (*B*, *E*, *F*, *H*, *K*, *M*, *N*, *O*, *P*, *R*, and *V*) days or in soil for 5 weeks (*C*, *D*, *I*, *J*, *S*, *T*, and *U*).

Table 1. Summary of expression patterns of nitrilase–GUS fusions

	Seedling (3–12 days)						Mature (5 weeks)					
			Leaf		Root							
Gene	Cotyledon	Hypocotyl	Tip	Vascular	Tip	Vascular	Leaf	Stipule	Stem	Sepal	Anther	Silique
NIT1	+	+	+	−	+	*	+	+	+	+	+	+
NIT2	+	*	−	−	*	−	−	+	−	*	−	+
NIT3	+	+	−	+	−	*	−	−	−	−	−	−
NIT4	*	−	+	−	+	−	+	+	+	+	*	+

+, staining in all Gus$^+$ transformants examined; *, weak staining in some transformants, no staining in others; −, no staining observed.

NIT2–GUS was expressed in the cotyledons (Fig. 4*G*), stipules (Fig. 4*H*), and root tips (Fig. 4*K*) of seedlings; in mature plants at the tip and the base of green siliques (Fig. 4 *I* and *J*), in some embryos (Fig. 4*J*), and weakly in pollen. NIT3–GUS was found in the vascular tissue of hypocotyls (Fig. 4*L*), cotyledons, leaves (Fig. 4 *M* and *N*), and roots (Fig. 4*O*) but was not detected in root tips (Fig. 4*P*) or reproductive structures. In seedlings, NIT4–GUS stained root tips (Fig. 4 *Q* and *V*) and the distal tip of young leaves (Fig. 4*R*), whereas in mature plants, it was detected in stems, cauline leaves, sepals (Fig. 4*S*), stipules, and at the tip and the base of siliques (Fig. 4 *T* and *U*). These results are summarized in Table 1.

The response of the nitrilase genes to pathogen infiltration was also investigated. Leaves infiltrated with an avirulent *Pseudomonas syringae* strain showed a modest induction of NIT2–GUS staining after 48 hr, whereas infiltration with a virulent strain led to a dramatic increase in NIT2–GUS staining at the bacterial lesions (Fig. 5). In contrast, NIT1–, NIT3–, and NIT4–GUS did not respond to pathogen infiltration (Fig. 5). This NIT2-specific induction following *P. syringae* infiltration was confirmed using Northern analysis with gene-specific probes (data not shown).

DISCUSSION

In *A. thaliana*, at least four genes encode nitrilases that can convert IAN to the auxin IAA *in vitro*. The sequences of these enzymes are similar to nitrilases from microorganisms, and a cysteine residue essential for microbial nitrilase activity (23, 25, 26) is conserved in all four *A. thaliana* nitrilases (Fig. 1). The most similar sequence in the GenBank data base (Release 81.0) to the *A. thaliana* nitrilases is a gene of unknown function from *Saccharomyces cerevisiae* (Fig. 1). The three *NIT* genes clustered on chromosome III are all more similar to each other than to *NIT4*, which is located on chromosome V. It is likely that *NIT1*, *NIT2*, and *NIT3* result from relatively recent gene duplications.

The nitrilase genes are differentially regulated *in vivo*, as assayed both by RNA gel blot analysis (Fig. 3) and promoter–reporter gene fusions (Figs. 4 and 5 and Table 1). These two methods for analyzing nitrilase tissue-specific expression are largely consistent for mature plants. For example, *NIT1* and *NIT4* mRNAs are detected in mature leaves and stems, and this is reflected in the GUS staining. Similarly, the absence of *NIT2* and *NIT3* expression in mature stems and flowers agrees with both methods. The analysis of GUS fusions provides a higher resolution view of the location and timing of expression within each tissue. For example, *NIT1*, *NIT2*, and *NIT4* mRNAs accumulate in siliques, and this is reflected by promoter-driven GUS expression in the silique tip and base. Moreover, whereas only *NIT1* and *NIT3* mRNAs are detected in roots of 5-week-old plants, in younger plants, all four nitrilase–GUS fusions are detected, with *NIT1*, *NIT2*,

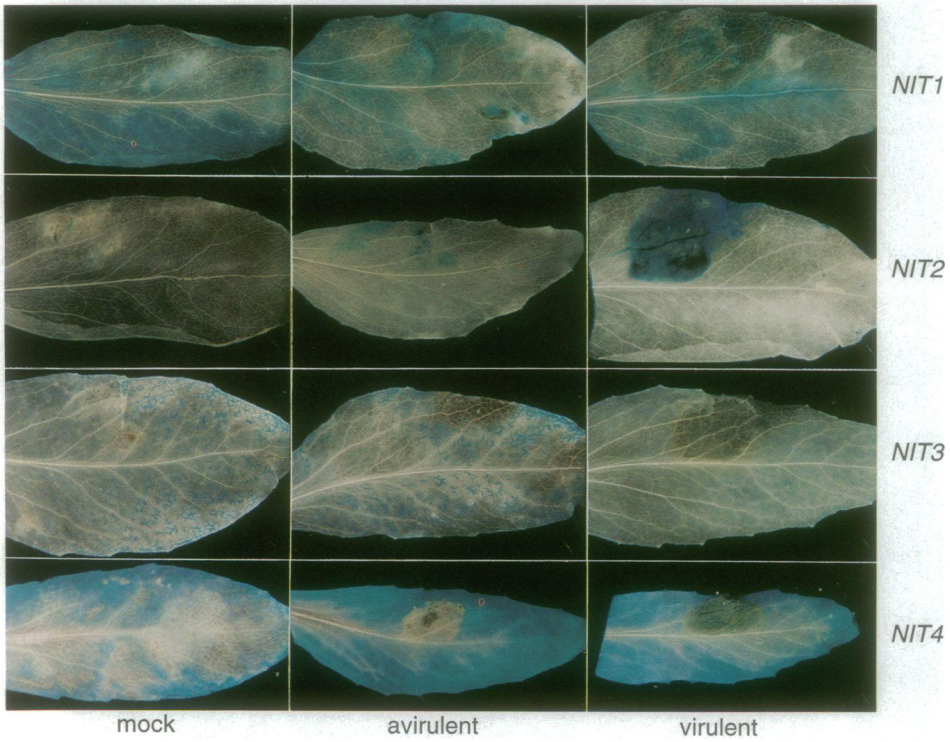

FIG. 5. Specific localized induction of NIT2–GUS by bacterial pathogen infiltration. Leaves of 3-week-old transgenic *A. thaliana* plants (*NIT1*, NIT1–GUS; *NIT2*, NIT2–GUS; *NIT3*, NIT3–GUS; *NIT4*, NIT4–GUS) were excised and stained for GUS activity 48 hr after inoculation with 10 mM $MgSO_4$ (mock), *P. syringae* pv. *tomato* MM1065 (avirulent), or *P. syringae* pv. *maculicola* ES4326 (virulent) as described (28).

and *NIT4* staining root tips and *NIT3* staining the root vasculature but not tips.

The sites of nitrilase expression may be sites of auxin biosynthesis in *A. thaliana*. Auxin is transported in an apical to basal direction (29), suggesting synthesis in distal tissues, such as tips of unexpanded leaves, where *NIT1* and *NIT4* are expressed (Fig. 4 *B* and *R*). In addition, root tips, where three nitrilase genes are expressed, are areas of active cell division, a process that is stimulated by auxin (30). Interestingly, when seedlings are germinated on high levels of IAN, adventitious roots are formed at the base of the hypocotyl (unpublished data), a region where NIT1–GUS is highly expressed (Fig. 4*A*). The pattern of nitrilase gene expression is partially overlapping with that of an *A. thaliana* auxin-inducible gene, *AtAux2-11*, monitored by promoter fusion to the reporter *lacZ* (31). Like the nitrilase genes, *AtAux2-11* is expressed in cotyledons, root tips, vascular tissue, stipules, sepals, and anthers and is absent from floral and vegetative meristems (31).

The specific induction of *NIT2*, which is normally only weakly expressed in vegetative tissue, by *P. syringae* infiltration (Fig. 5) parallels pathogen induction of genes in the tryptophan pathway (12, 32) and implies a role for auxin in defense against pathogens.

Further study of substrate specificity is required to determine which nitrilase isozymes are primarily responsible for auxin biosynthesis *in vivo*. Quantitation of IAA and IAN in transgenic plants that overproduce each nitrilase cDNA in sense and antisense orientations should provide direct evidence as to whether IAN serves as an IAA precursor in *A. thaliana*.

We gratefully acknowledge K. Niyogi for RNA; J. Bender, B. Keith, and K. Niyogi for DNA from F_2 plants; J. Celenza for advice on transformation; J. Mulligan, S. Elledge, R. Davis, and F. Lacroute for libraries; and J. Bender, J. Celenza, A. Diener, J. Loeb, S. Matsuda, and E. Vierling for comments on the manuscript. B.B. was supported by a postdoctoral fellowship from the American Cancer Society and G.R.F. is an American Cancer Society Professor of Genetics. This research was supported by a grant from the National Science Foundation (MCB9317175).

1. Klee, H. & Estelle, M. (1991) *Annu. Rev. Plant Physiol. Plant Mol. Biol.* **42**, 529–551.
2. Ludwig-Müller, J. & Hilgenberg, W. (1988) *Physiol. Plant.* **74**, 240–250.
3. Thimann, K. V. & Mahadevan, S. (1964) *Arch. Biochem. Biophys.* **105**, 133–141.
4. Rausch, T. & Hilgenberg, W. (1980) *Biochemistry* **19**, 747–750.
5. Bartling, D., Seedorf, M., Mithöfer, A. & Weiler, E. W. (1992) *Eur. J. Biochem.* **205**, 417–424.
6. Normanly, J., Cohen, J. D. & Fink, G. R. (1993) *Proc. Natl. Acad. Sci. USA* **90**, 10355–10359.
7. Wright, A. D., Sampson, M. B., Neuffer, M. G., Michalczuk, L., Slovin, J. P. & Cohen, J. D. (1991) *Science* **254**, 998–1000.
8. Last, R. L. & Fink, G. R. (1988) *Science* **240**, 305–310.
9. Last, R. L., Bissinger, P. H., Mahoney, D. J., Radwanski, E. R. & Fink, G. R. (1991) *Plant Cell* **3**, 345–358.
10. Ooms, G., Hooykaas, P. J. J., van Veen, R. J. M., van Beelen, P., Regensburg-Tuïnk, T. J. G. & Schilperoort, R. A. (1982) *Plasmid* **7**, 15–29.
11. Ausubel, F. M., Brent, R., Kingston, R. E., Moore, D. D., Seidman, J. G., Smith, J. A. & Struhl, K., eds. (1993) *Current Protocols in Molecular Biology* (Greene and Wiley, New York).
12. Niyogi, K. K. & Fink, G. R. (1992) *Plant Cell* **4**, 721–733.
13. Church, G. M. & Gilbert, W. (1984) *Proc. Natl. Acad. Sci. USA* **81**, 1991–1995.
14. Elledge, S. J., Mulligan, J. T., Ramer, S. W., Spottswood, M. & Davis, R. W. (1991) *Proc. Natl. Acad. Sci. USA* **88**, 1731–1735.
15. Minet, M., Dufour, M.-E. & Lacroute, F. (1992) *Plant J.* **2**, 417–422.
16. Kosambi, D. D. (1944) *Ann. Eugen.* **12**, 172–175.
17. Lister, C. & Dean, C. (1993) *Plant J.* **4**, 745–750.
18. Konieczny, A. & Ausubel, F. M. (1993) *Plant J.* **4**, 403–410.
19. Jefferson, R. A., Kavanagh, T. A. & Bevan, M. W. (1987) *EMBO J.* **6**, 3901–3907.
20. Valvekens, D., Van Montagu, M. & Van Lijsebettens, M. (1988) *Proc. Natl. Acad. Sci. USA* **85**, 5536–5540.
21. Haughn, G. W. & Somerville, C. (1986) *Mol. Gen. Genet.* **204**, 430–434.
22. Castle, L. A. & Morris, R. O. (1990) *Plant Mol. Biol. Rep.* **8**, 28–39.
23. Kobayashi, M., Izui, H., Nagasawa, T. & Yamada, H. (1993) *Proc. Natl. Acad. Sci. USA* **90**, 247–251.
24. Higgins, D. G. & Sharp, P. M. (1989) *Comput. Appl. Biosci.* **5**, 151–153.
25. Kobayashi, M., Komeda, H., Yanaka, N., Nagasawa, T. & Yamada, H. (1992) *J. Biol. Chem.* **267**, 20746–20751.
26. Kobayashi, M., Yanaka, N., Nagasawa, T. & Yamada, H. (1992) *Biochemistry* **31**, 9000–9007.
27. Cherry, J. M., Cartinhour, S. W. & Goodman, H. M. (1992) *Plant Mol. Biol. Rep.* **10**, 308–309, 409–410.
28. Dong, X., Mindrinos, M., Davis, K. R. & Ausubel, F. M. (1991) *Plant Cell* **3**, 61–72.
29. Okada, K., Ueda, J., Komaki, M. K., Bell, C. J. & Shimura, Y. (1991) *Plant Cell* **3**, 677–684.
30. Blakely, L. M. & Evans, T. A. (1979) *Plant Sci. Lett.* **14**, 79–83.
31. Wyatt, R. E., Ainley, W. M., Nagao, R. T., Conner, T. W. & Key, J. L. (1993) *Plant Mol. Biol.* **22**, 731–749.
32. Keith, B., Dong, X., Ausubel, F. M. & Fink, G. R. (1991) *Proc. Natl. Acad. Sci. USA* **88**, 8821–8825.